Organic &
Biomolecular
Chemistry

rsc.li/obc

Volume 15
Number 47
21 December 2017
Pages 9945-10124

ISSN 1477-0520

ROYAL SOCIETY
OF CHEMISTRY

PAPER
I. J. Dmochowski et al
Oligonucleotide modifi cations enhance probe stability for
single cell transcriptome in vivo analysis (TIVA)

ROYAL SOCIETY
OF CHEMISTRY

rsc.li/obc

ARTICLE

Looking at the big picture in ASM/EDA analysis: the case of the *ortho-para* regioselectivity rule in Diels-Alder reactions

Nicolás Grimblat* and Ariel M. Sarotti*

The regioselectivity of the Diels-Alder reaction is predicted by the *ortho-para* rule which has been explained from FMO theory. Using DFT calculations, the activation-strain model and energy decomposition analysis we studied the reaction of methyl acrylate with four unsymmetrical dienes. We found that if the analysis is carried out considering the TS structures, the selectivity would not be explained by the interaction energy as expected considering the FMO arguments. However, a thorough analysis along the reaction path revealed that the interaction energy is responsible for the regioselectivity. A deeper analysis with the EDA model showed that the decisive term that accounts for the HOMO-LUMO interactions favors the *ortho* and *para* paths, as predicted by FMO arguments.

Introduction

The Diels-Alder (DA) reaction is one of the most important and deeply studied chemical reactions of all times, both theoretically and experimentally.[1–3] One of the main features is the possibility to generate up to 4 stereocenters in a stereospecific and regioselective manner. In the case of unsymmetrical dienes and dienophiles, the regioselectivity of the process can be easily predicted through the well-known "*ortho-para*" rule (Scheme 1a).[4] This preference has been explained from classic Fukui's frontier MO (FMO) theory arguments, on the basis of the influence of the substituents in the coefficients of the interacting orbitals.[5–7] Conceptual DFT theory offers an alternative picture, with the regioselectivity arising from the favoured bonding of the most nucleophilic and electrophilic centres of the two fragments.[8] In any case, both approaches suggest that a more efficient binding between fragments should account for the selectivity. However, the regioselectivity of a kinetically controlled reaction is determined by the energy of the competing transition structures (TS), which being significantly distorted in relation with the isolated reagents, might afford different MOs. Therefore, a more realistic examination should consider the interaction between orbitals of the distorted fragments at the TSs.

The Distortion/Interaction-Activation Strain Model (D/I-ASM) developed by Houk and Bickelhaupt, respectively,[9–11] provides a third and more comprehensive option to shed light on reactivity and selectivity issues of chemical reactions.[12–15] In this fragment-based approach the potential energy surface $\Delta E(\zeta)$ is decomposed along the reaction coordinate ζ into two terms: the strain $\Delta E_{strain}(\zeta)$ resulting from the distortion of the individual reactants and the interaction $\Delta E_{int}(\zeta)$ between the distorted reactants. This last term can be further partitioned with the Energy Decomposition Analysis (EDA) into three physically meaningful terms, namely ΔV_{elstat} (Coulombic interaction), ΔE_{Pauli} (steric repulsion) and ΔE_{oi} (orbital bonding, accounting for HOMO-LUMO interactions, polarization and SOI).[16]

This model has been successfully invoked for a wide variety of reactions, such as additions,[17–19] organometallic[20–22] and cycloadditions.[14,23–28] In the particular case of the DA reaction, the D/I-ASM model was employed to understand underlying characteristics such as the "*endo rule*" and reactivity,[2,9,36,24,29–35] as well as other regioselectivity aspects (such as those related with intramolecular processes, arynes or fullerenes).[26,37–40]
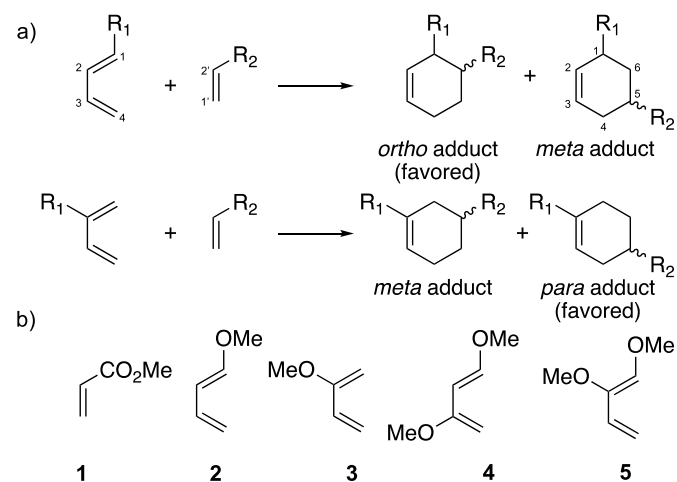
Scheme 1.

Scheme 1. a) Schematic representation of the *ortho-para* rule; b) Dienes and dienophile considered in this study.

Surprisingly, to the best of our knowledge, the origins of the *ortho-para* rule have not been unravelled by means of D/I-ASM. Merging the FMO arguments into D/I-ASM logic, it is envisaged that the preferred regioisomer might account for a path where there is a more stabilizing interaction for this approach. However, distortion has been pointed as the most influential factor in related chemical processes.[15,41,42] In an effort to account for the role of such terms in dictating the *ortho-para* rule, we evaluated the DA reaction of unsymmetrical dienes (**2-5**) with methyl acrylate (**1**) at the M06-2X/def2-TZVPP level of theory for all optimizations, D/I-ASM and EDA.[43,44]

Computational Methods

Geometry optimization of all stationary points was performed using Gaussian 09, revision C.01,[45] employing the meta-hybrid M06-2X exchange-correlation functional using the triple-ζ quality plus polarization def2-TZVPP basis set. Analytical frequency calculations were performed to characterize the nature of the stationary points. The reactants and the cycloadducts showed real frequencies indicating their location on the potential-energy surface (PES) as local minima, while the transition state (TS) showed one imaginary frequency. The PES of the reaction was obtained by performing intrinsic reaction coordinate (IRC) calculations. Single-point energy were calculated at the same level of theory. All calculations were performed using Gaussian 09, revision C.01 default numerical settings. The distortion/interaction-activation strain model (D/I-ASM) analysis was performed using ADF.2016 program[46] at the M06-2X/TZ2P // M06-2X/def2-TZVPP level of theory. Optimized structures were illustrated using CYLview.[47]

Results

Monosubstituted dienes

We started by exploring the DA reaction of **1** with 1-methoxy-1,3-butadiene (**2**) and 2-methoxy-1,3-butadiene (**3**), which give rise exclusively to the *ortho-* and *para-* substituted cyclohexenes, respectively.[48,49] This makes these dienes perfect to unveil the origin of the regioselectivity corresponding to the DA reactions. The calculated selectivities for both approaches (99:1, $\Delta\Delta G^{\neq} = \sim$2.6 kcal/mol) nicely agreed with the observed experimental trends, supporting the selected computational methodology (Figure 1).

To decipher the differences in the activation energies for the competing TSs, a D/I-ASM was applied along the intrinsic reaction coordinate defined by the average distance of both C-C forming bonds. This analysis was initially performed at the corresponding transition structures for each regioisomer within each reaction (Figure 2). Unexpectedly, we found that for the TSs of **1**+**2** the preference for the *ortho* adduct lies on the distortion of the system ($\Delta\Delta E^{\neq}_{strain}$ = 2.5 kcal/mol) and not on the interaction as we would have expected based on FMO arguments ($\Delta\Delta E^{\neq}_{int} \sim$ 0.0 kcal/mol).[5] In contrast, for **1**+**3** both isomers have *ca.* the same distortion value at the TS, making the

interaction responsible for the stabilization towards the observed selectivity ($\Delta\Delta E^{\neq}_{int}$ = 2.7 kcal/mol), which is in line with the FMO theory. This could be rationalized by the fact that when the later diene reacts, the substituted position is not involved in the newly formed σ bonds, hence it maintains its sp^2 hybridization along the reaction path minimizing any deformation. On the other hand, C_1 is the carbon atom bearing
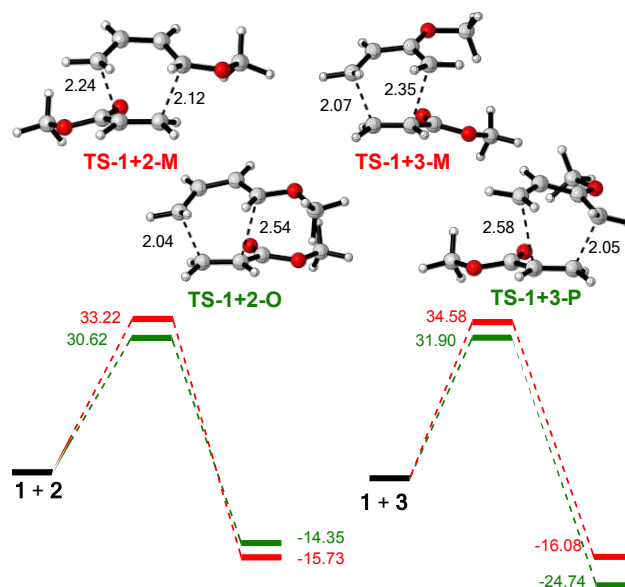

Figure 1. Computed reaction profiles for the reactions of **2** and **3** with **1**. Gibbs energies in kcal/mol and distances in Å.

the substituent for **2,** which modifies its hybridization to sp^3 in the final cycloadduct.

Although this approach considering the transition structures has been extensively employed in the past, it has recently been proved that the analysis only at this point might give rise to misleading results, identifying different energy components responsible for the observed reactivity or selectivity trends.[10,36,50] This is particularly true when TSs shift from early to late TS, as occur in the reactions under study, where the favoured *ortho* and *para* approximations have earlier TSs and are more exergonic than their *meta* counterparts. This change to a less exergonic and later transition structure is in accordance with the Hammond postulate. To overcome this issue, the analysis terms should be computed at a consistent geometry, *i.e.* at the same average distance of the newly forming C-C bonds.

Due to the controversial results found for **2**, we carried out the same study at the same average distance ($\sim$2.2Å). In this fashion, it became clear that it is not the distortion but the interaction the term controlling the regioselectivity ($\Delta\Delta E_{strain}$ = 20.8 and $\Delta\Delta E_{int}$ = -26.8 kcal/mol for **2** and $\Delta\Delta E_{strain}$ = 20.0 and $\Delta\Delta E_{int}$ = -25.9 kcal/mol for **3**). This is because the position of the TS causes the ΔE correlate with the ΔE_{strain} and not the ΔE_{int}. This result is in agreement with FMO and enhance the importance of the analysis along the reaction path.

To gain deeper insights, we used the EDA method to further understand the effect of the interaction factor that gives the experimental selectivity (Figure 2). Interestingly, the analysis at the TS for both dienes showed that the $\Delta E^{\neq}_{oi}$ term (accounting

Journal Name

ARTICLE

for the HOMO-LUMO interactions among others) destabilize the favoured adduct by ~2.3 kcal/mol. In the case of **2**, also the electrostatic term stabilizes the *meta* cycloadduct (both terms account for a total of 4.3 kcal/mol), while for **3** this factor slightly favours the *para* isomer, stabilizing the *meta* adduct by 1.9 kcal/mol overall. In both reactions, the *meta* TSs are more crowded leading to higher Pauli repulsion and making it the main energy term that accounts for the overall interaction values (Table 2). In a more complete form, the Steric term (the combination of Pauli and electrostatic terms) is responsible of the observed selectivity in the case of **3**, destabilizing the *meta* channel by 5.01 kcal/mol. On the other hand, this term offsets the stabilizing effect of the $\Delta E^{\neq}_{oi}$ term, leading to the almost null $\Delta\Delta E^{\neq}_{int}$ in **1**+**2**.

However, these counterintuitive results considering the widely accepted FMO viewpoint (which suggests that the interaction between the HOMO-LUMO pair accounts for the regioselectivity)[2] were observed when the analysis of this models was made on the TSs. According to these findings, the FMO approach would only be reflected at the beginning of the reaction path.

When the interaction was analysed through ASM at the same average C-C forming distance, the role of the orbital interaction and to a lesser extent the electrostatic interaction could be identified as the determining trends for the interaction energy ($\Delta\Delta E_{oi}$ = -51.7 and $\Delta\Delta V_{elstat}$ = -25.5 kcal/mol for **2** and $\Delta\Delta E_{oi}$ = -45.6 and $\Delta\Delta V_{elstat}$ = -26.1 kcal/mol for **3**). These results, unlike the previous ones based on the TSs, support the long-established findings of FMO. The orbital interaction, which accounts for the HOMO-LUMO, is responsible for the regioselectivity of the DA reactions.

Both reactions were found to be normal Diels-Alder reactions, since the $HOMO_{diene}$-$LUMO_1$ gap has a value of 6.77 eV for **2**, and 7.21 eV for **3**, while the $HOMO_1$-$LUMO_{diene}$ gaps are 10.13 eV and 9.80 eV for **2** and **3**, respectively. The analysis using Kohn-Sham molecular orbital analysis at the average C-C bond formation of ~2.2 Å, revealed that the favoured approach has a gap of 5.1 eV for the *ortho* adduct and of 5.44 eV for the *para* adduct, being the gap for their respective counterparts of 5.83 eV and 6.23 eV, respectively. Additionally, we performed an analysis of the overlap at the same C-C forming bond distance for both approaches. It is worth underline that this study is

carried out only with the *endo* adducts. Since are both normal demand DA reactions, the analysis of the $HOMO_{diene}$-$LUMO_1$ showed that for **2** there is a difference in the overlap of 0.03 favouring the *ortho* adduct. For **3**, this interaction exhibited a difference of 0.02 in favour of the *para* isomer. These differences between the HOMO of the dienes and the LUMO of the dienophile is expected since there is a better overlapping of the reactive lobes; the one in the δ position for **2** (substituted in the α position) and the one in the α position for **3** (substituted in the β position).

Table 1. Orbital Overlap (*S*)

		FMO Interaction[a]	
		$HOMO_d$ – $LUMO_1$	$HOMO_1$ - $LUMO_d$
1+2	*Meta*	0.20	0.21
	Ortho	0.23	0.21
1+3	*Meta*	0.22	0.19
	Para	0.24	0.21
1+4	*Meta/Meta*	0.19	0.20
	Ortho/Para	0.23	0.19
1+5	*Meta/Para*	0.20	0.21
	Ortho/Meta	0.20	0.20

[a] d = diene

All these results showed that if we would base our conclusions on the analysis of the TSs, we would be questioning the long stablished FMO theory. These observations highlight the evidences of previous studies, where the TS may provide misleading information.

Disubstituted dienes

With these results in hand, we decided to extend the grounds of this study to model the reactions of 1,3-dimethoxy-1,3-butadiene (**4**) which is an analogue of the Danishefsky's diene, and the 1,2-dimethoxy-1,3-butadiene (**5**). These disubstituted dienes, which could be seen as the two possible chimeras of **2** and **3**, were selected to offer two different scenarios. In the case of **4**, a high regioselectivity should be expected given the reinforced effect exerted by the two methoxy groups at C_1 and C_3 (*ortho* and *para* directing, respectively). On the other hand, the mismatched directing trends in **5** would afford an interesting case study to analyse the competing orbital effect in the diene. The thorough study of these systems will provide a deeper and better understanding of this rule due to this "enhanced" and "opposite" effects due to the position of the substituents in the reacting orbitals of the diene.

Table 2. D/I-ASM and EDA energies (in kcal/mol) for all DA reactions under study.

	1+2			**1+3**			**1+4**			**1+5**		
	Meta	*Ortho*	$\Delta\Delta E^{\neq[a]}$	*Meta*	*Para*	$\Delta\Delta E^{\neq[a]}$	*Meta/Meta*	*Ortho/Para*	$\Delta\Delta E^{\neq[a]}$	*Meta/Para*	*Ortho/Meta*	$\Delta\Delta E^{\neq[a]}$
$\Delta E^{\neq}$	17.5	15.0	2.6	18.5	15.9	2.6	17.3	11.6	5.7	9.9	7.8	2.1
$\Delta E^{\neq}_{strain}$	30.9	28.4	2.5	29.8	29.9	-0.1	32.9	27.1	5.8	25.6	24.6	1.0
$\Delta E^{\neq}_{int}$	-13.4	-13.5	0.0	-11.4	-14.1	2.7	-15.6	-15.5	-0.1	-15.7	-16.8	1.1
$\Delta V^{\neq}_{elstat}$	-54.0	-52.0	-2.0	-54.6	-55.1	0.5	-57.2	-56.1	-1.2	-52.9	-52.1	-0.9
$\Delta E^{\neq}_{oi}$	-62.1	-59.8	-2.3	-61.4	-59.1	-2.4	-61.4	-59.0	-2.3	-58.0	-56.6	-1.3
$\Delta E^{\neq}_{Pauli}$	103.0	98.7	4.3	104.9	100.5	4.5	103.3	99.9	3.4	95.6	92.5	3.1

[a] $\Delta\Delta E_i^{\neq}$ = $\Delta E_i^{\neq}{}_{unfavored}$ - $\Delta E_i^{\neq}{}_{favored}$
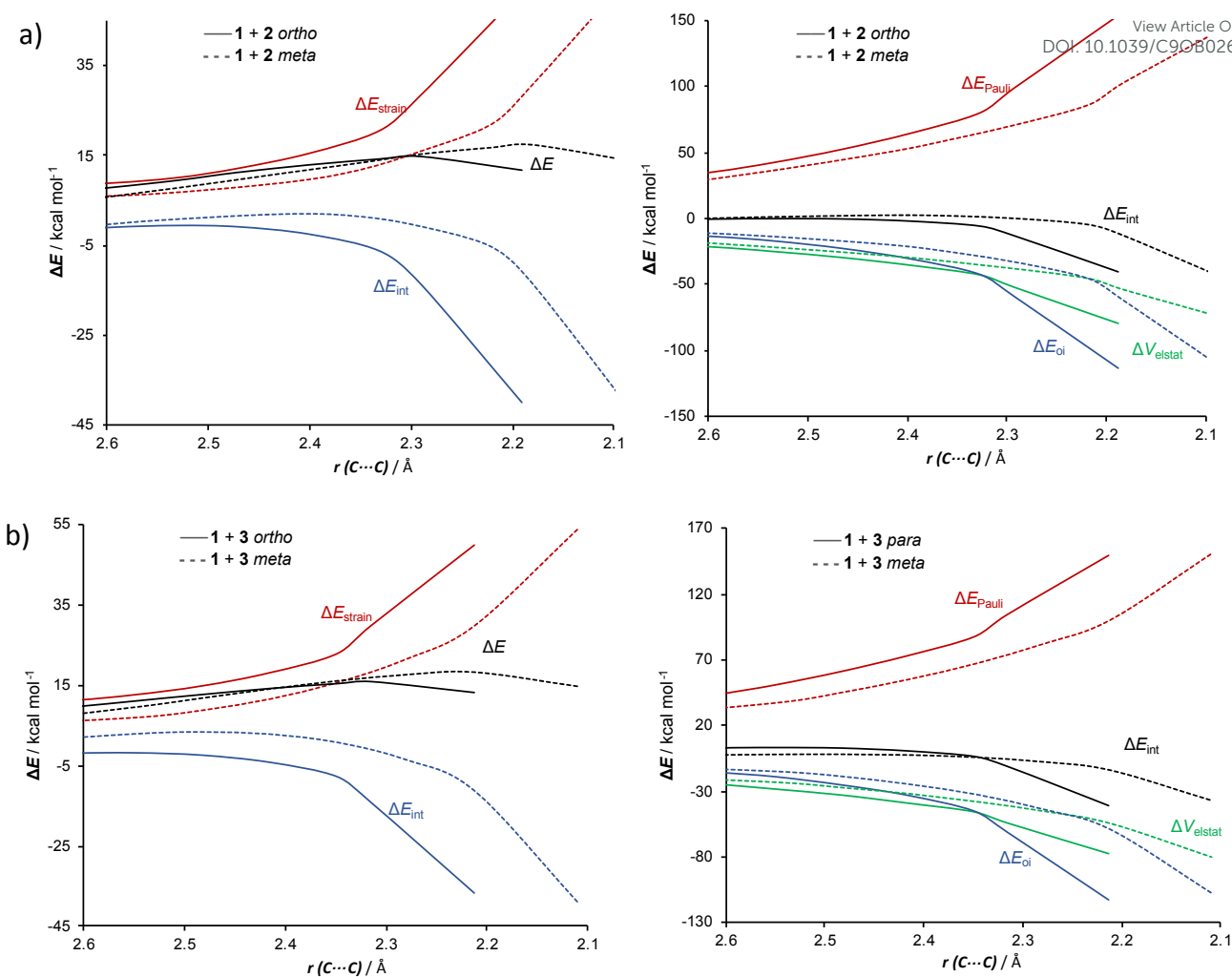
Figure 2. ASD (left) and decomposition of the interaction energy diagram (right) of a) **1** + **2** and b) **1** + **3**. The markers highlight the position of the TS.

Table 3. D/I-ASM and EDA energies (in kcal/mol) for all DA reactions under study at 2.2Å.

	1+2			1+3			1+4			1+5		
	Ortho	Meta	$\Delta\Delta E$ [a]	Para	Meta	$\Delta\Delta E$ [a]	Ortho/Para	Meta/Meta	$\Delta\Delta E$ [a]	Ortho/Meta	Meta/Para	$\Delta\Delta E$ [a]
ΔE	11.8	17.5	-5.7	13.2	18.5	-5.3	8.7	17.3	-8.5	6.0	9.2	-3.2
ΔE_{strain}	51.8	30.9	20.8	49.8	29.8	20.0	53.1	32.9	20.2	40.7	35.1	5.6
ΔE_{int}	-39.9	-13.1	-26.8	-37.0	-11.1	-25.9	-45.0	-15.3	-29.7	-34.1	-25.5	-8.6
ΔV_{elstat}	-79.5	-54.0	-25.5	-80.6	-54.6	-26.1	-99.3	-57.2	-42.1	-70.3	-63.2	-7.1
ΔE_{oi}	-113.8	-62.1	-51.7	-107.1	-61.4	-45.6	-131.7	-61.4	-70.4	-92.3	-77.5	-14.8
ΔE_{Pauli}	153.4	103.0	50.4	150.7	104.9	45.8	186.1	103.3	82.8	128.5	115.2	13.2

[a] $\Delta\Delta E_i = \Delta E_{i\text{-favored}} - \Delta E_{i\text{-unfavored}}$

For **4**, the products of the DA reaction with methyl acrylate can be *ortho-para* or *meta-meta* substituted cycloadducts, where the first is predicted by the regioselectivity rule under study, since it is favoured by both substitution positions. As expected, our calculations showed that the *ortho-para* adduct is formed exclusively (>99:1, $\Delta\Delta G^{\neq} > 6$ kcal/mol).[51] In line with the previous observations, the unfavoured approach have late transition structures with higher activation barrier, in agreement with the Hammond–Leffer postulate.

The D-I/ASM analysis depicted by the Activation Strain Diagrams (ASDs) (Figure 4) showed that the selectivity trend is mainly due to distortion ($\Delta\Delta\Delta E^{\neq}_{strain} = 5.8$ kcal/mol), whereas

almost no difference in the interaction factor was noticed ($\Delta\Delta\Delta E^{\neq}_{int} = 0.1$ kcal/mol). This is true when we compared both approaches at the transition structures. Once again, calculating these energies at the TSs provide FMO challenging results. However, if we compared the competing mechanisms along the reaction path and performed the analysis at ~2.2Å, we observed that the interaction is responsible for this difference, with a $\Delta\Delta E_{strain}$ of 20.2 kcal/mol and $\Delta\Delta E_{int}$ of -29.7 kcal/mol. According to this approach, the interaction is the responsible of the difference in energy that gives rise to the selectivity observed experimentally for electron rich 1,3-disubstituted dienes. As

previously observed, the results of this approach return energetic values in agreement with FMO theory.

We expected that the analysis of the EDA would shed light on the stabilization values of the interaction energy (Table 2). Analysing the breakdown of this term we observed that if we consider the TS structures, both approaches have approximately the same values of stabilizing components ($\Delta\Delta E^{\neq}_{oi}$ and $\Delta\Delta V^{\neq}_{elstat}$ = -2.3 and -1.2 kcal/mol, respectively) and the difference is arise from the $\Delta\Delta E^{\neq}_{Pauli}$ (3.4 kcal/mol). A deeper analysis through reaction path at the same average C···C bond distance (~2.2Å), revealed different results. From this perspective, the orbital interaction ($\Delta\Delta E^{\neq}_{oi}$ = -70.4 kcal/mol) and to a lesser extent the electrostatic interaction ($\Delta\Delta V^{\neq}_{elstat}$ = -42.1 kcal/mol) are responsible for the overall interaction energy value. Once again, this approach is consistent with the predictive FMO theory for the DA reactions.

Regarding FMO, the analysis of the corresponding HOMO and LUMO orbitals of both diene and dienophile was in agreement with the expected results. Within the reactants, there is a HOMO$_4$-LUMO$_1$ gap of 6.83 eV, stating that this is a normal DA reaction since HOMO$_1$-LUMO$_4$ has a value of 10.32 eV. At the consistent considered geometry of ~2.2Å, the best orbital interaction arises from HOMO$_{diene}$-LUMO$_{dienophile}$ and are in line with the selectivity, being the gap 4.68 eV for the *ortho/para* adduct and 5.58 eV for the *meta/meta* counterpart. The orbital overlap (*S*) showed almost no difference when the analysis is made with the HOMO$_{dienophile}$-LUMO$_{diene}$ which would be expected since it includes the secondary orbital interaction (SOI) and this analysis is carried out with both *endo* transition structures. A difference of 0.04 was observed when the inverse analysis (HOMO$_{diene}$-LUMO$_{dienophile}$) was made. This is due to the fact that substituents in both the 1- and 3- positions reinforce the reactive lobe for the diene, hence a better interaction between orbitals for the *ortho/para* addition.[2]
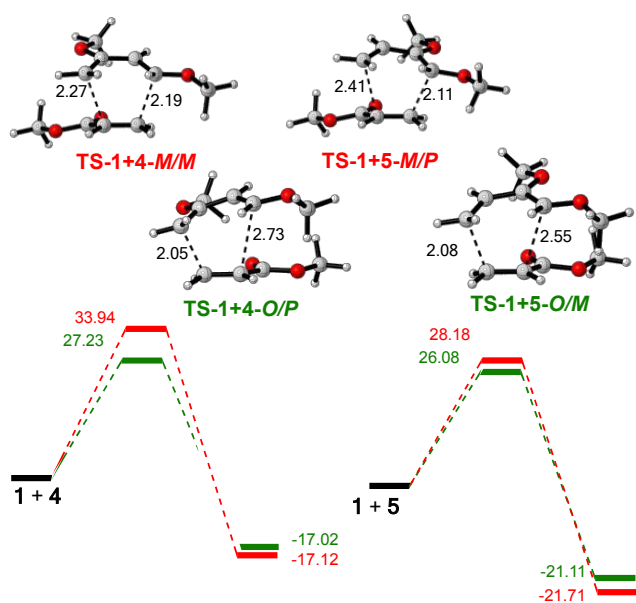

Figure 3. Computed reaction profiles for the reactions of **4** and **5** with **1**. Gibbs energies in kcal/mol and distances in Å.

The analysis of **5** is appealing since unlike all the previously studied dienes, there are competing effects based on the substituent positions. Given that this diene is 1,2 substituted there is a competing increase in the lobes of C$_1$ (due to the β-substituent) and C$_4$ (due to the α substituent). The products of the DA reaction can be *ortho-meta* or *meta-para*. Unfortunately the DA reaction for this diene do not exist on the literature, but it can be considered an analogue of the 3-methyl-1,3-pentadiene that do exists.[52] For this reaction, we found that the *ortho/meta* path is favoured with a selectivity of 95:5 ($\Delta\Delta G^{\neq}$ = 2.1 kcal/mol), consistent with the methyl substituted diene. As observed for all other dienes under study the unfavoured approach has a later transition structure and higher activation barrier. However, in this situation, the difference is not as marked as for the other dienes ($\Delta d^{\neq}_{C-C}$ = 0.06Å for this diene and > 0.1Å for the other dienes).

The DA reaction of **5** presented decomposition energies that showed that the *ortho-meta* TS is favoured both by the interaction and distortion ($\Delta\Delta E^{\neq}_{int}$ and $\Delta\Delta E^{\neq}_{strain}$ = 1.1 and 1.0 kcal/mol, respectively). Hence, unlike the other dienes under study, the regioselectivity is given by the combination of both factors. This analysis on the TS compared with the analysis on the TS of **2** and **3**, are in agreement since they are defined by distortion and interaction, respectively. However, we performed the analysis at ~2.2Å for both approaches, we observed that the interaction is the only responsible for the observed selectivity ($\Delta\Delta E_{strain}$ of 5.6 kcal/mol and $\Delta\Delta E_{int}$ of -8.6 kcal/mol). It is really interesting that for this diene the $\Delta\Delta E$ of both terms is considerably lower than for the other dienes ($\Delta\Delta\Delta E_{strain}$ > 14 and $\Delta\Delta\Delta E_{int}$ > 16 kcal/mol). This is in line with the expected results based on the FMO theory, since the substituents in this diene present an opposite activation pattern.

The EDA analysis performed with the transition structures showed a pattern similar to that observed for **4**, where both orbital and electrostatic terms are more stabilizing for the unfavoured cycloadduct ($\Delta\Delta E^{\neq}_{oi}$ and $\Delta\Delta V^{\neq}_{elstat}$ = -1.3 and -0.9 kcal/mol, respectively). The Pauli repulsion term is the key factor that compensate those other terms that support the *meta/para* isomer by 3.1 kcal/mol. However, when we carried out this analysis at the consistent average C-C bond distance of ~2.2Å, we observed that it is not the Pauli but the Orbital interaction and electrostatic terms the ones that account for the regioselectivity ($\Delta\Delta E^{\neq}_{oi}$ and $\Delta\Delta V^{\neq}_{elstat}$ = -14.8 and -7.1 kcal/mol, respectively). It seems important to highlight the fact that the $\Delta\Delta E$ value for both terms are at least a third of the corresponding values for any other diene under study. Once again, this is a clear reflection of the competitiveness of this system.

Nonetheless, the observed trend and selectivity is in agreement with the FMO since the presence of a substituent in both 1- and 2- positions have an opposite effect; the substituent in the α position increases the lobe of the δ position, while the substituent in the β position does the same for the α position.[4] Therefore, since they are not aligned, or they "do not favour the same reactive site" the interaction between the FMO does not stabilize the system as much as it does for the other systems.

ARTICLE

Journal Name

The analysis of this FMO, proved that this is a normal DA reaction, since the $HOMO_5$-$LUMO_1$ has a gap of 6.67 eV and the gap for the $HOMO_5$-$LUMO_1$ is 9.91 eV. The analysis of this interaction at ~2.2Å is in agreement with the selectivity for this reaction, having a $HOMO_{diene}$-$LUMO_{dienophile}$ gap of 4.87 eV for the *ortho/meta* and of 5.02 eV for the *meta/para* regioisomer. As previously observed, the difference of the calculated values to unveil the origin of the selectivity for this diene, is at least a third of the values observed for the other dienes. Considering the "mismatch" of the substituents on the diene, it is reasonable that the orbital overlap shows no difference, regarding the FMO considered.

It is well known that the interaction of the FMOs with higher coefficients leads to more asynchronous TSs,[5] *i.e.* the forming bond that corresponds to the favourable FMO interaction is shorter, which in turn makes this distance smaller in order to maximize the orbital stabilization. This suggests that the reactants in the favoured reactions distort further (have higher distortion energies along the IRC) in order to maximize the stabilizing orbital interactions, which gets reflected on the higher asynchronicity. All these observations and results obtained through this analysis support the FMO theory statements, denoting the different activation of the diene based on the substitution pattern.

This work also reinforces the fact that the results performed only at the TSs may lead to different and counterintuitive conclusions. The analysis should be carried out meticulously through all the reaction path, where the true origin of selectivities or reactivities can be unveiled. It is particularly important in cases where there is a shift from early to late TS as is the situation in this study.
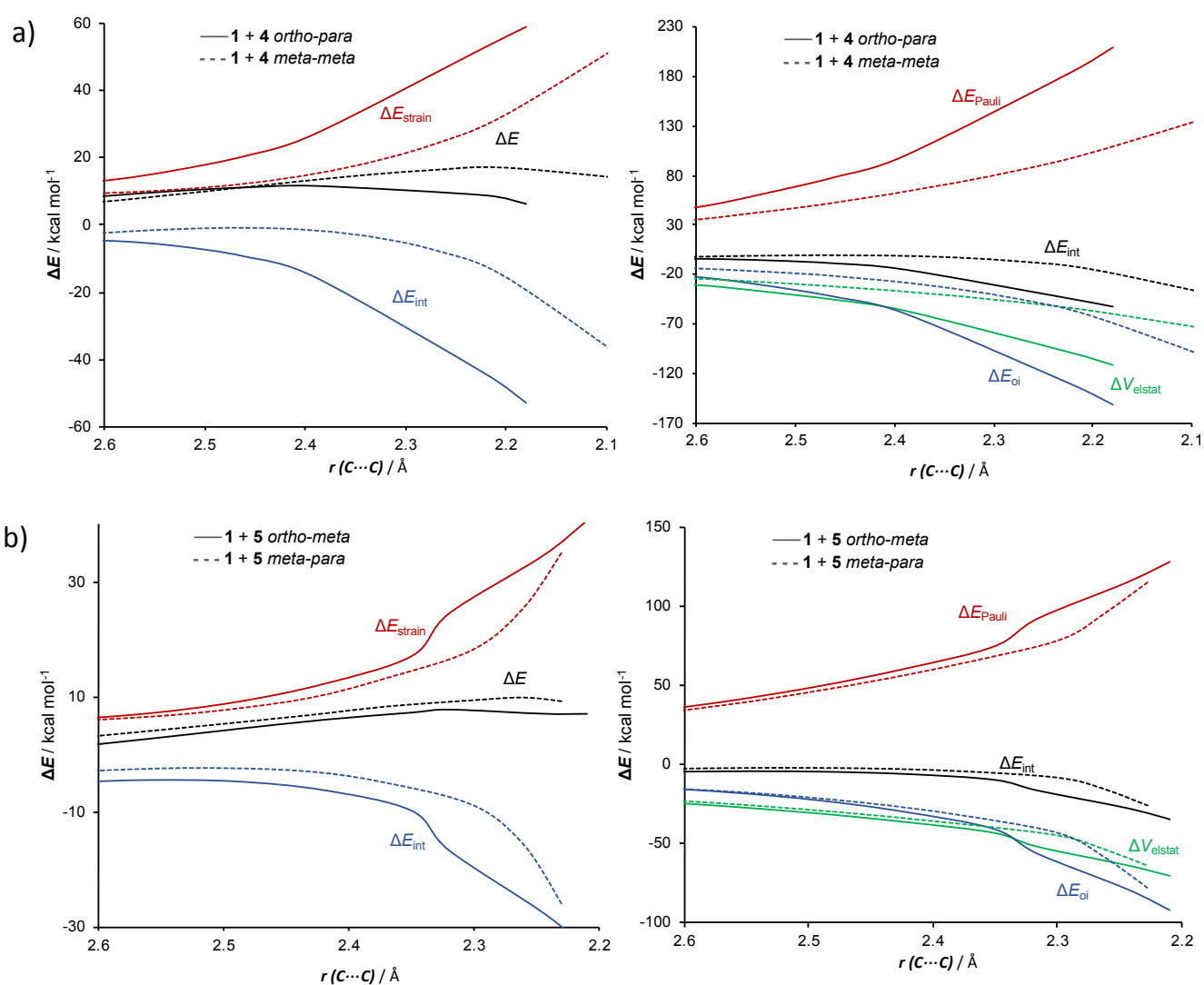

Figure 4. ASD (left) and decomposition of the interaction energy diagram (right) of a) **1** + **4** and b) **1** + **5**

ARTICLE

Conclusions

With the intention of gaining a deeper insight on the origins of the regioselectivity observed in the DA reaction we performed a D/I-ASM and EDA analysis to understand the factors governing this rule. We found that all dienes under study presented energetic components consistent with those corresponding to the FMO theory. The interaction is found to be the term accounting for the regioselectivity observed experimentally, regardless the substitution pattern. Particularly, the distortion of each system is a consequence of the spatial arrangement that maximizes the orbital interaction.

It was found that the key on the observed trend is the orbital interaction and to a lesser extent the electrostatic terms. This nicely agreed with the expected results, since the orbital interaction accounts for the interaction of the HOMO-LUMO (*i.e*. correlates with the FMO theory). The analysis of **5** prove to be an interesting and particular challenge since there is a mismatch substitution pattern (activation of reactive orbitals), which is reflected in the small difference in every energetic term for both approximations.

A concluding remark considering all of the observations presented herein, and the vast literature in this area is that to precisely carry out a study with these models, the analysis only at the transition structures of each system may lead to counterintuitive and incorrect results. This is the reason the analysis should be performed along the reaction path, to truly answer the questions that lead to perform a research employing this methodology.

In this particular study, if the analysis was not performed at the average distance of both C-C forming bonds of 2.2Å, our conclusions we would be different. Instead of obtaining results in line with FMO, we would be questioning this long-stablished theory.

Conflicts of interest

In accordance with our policy on Conflicts of interest please ensure that a conflicts of interest statement is included in your manuscript here. Please note that this statement is required for all submitted manuscripts. If no conflicts exist, please state that "There are no conflicts to declare".

Acknowledgements

Notes and references

1   F. Fringuelli and A. Taticchi, *The Diels-Alder Reaction: Selected Practical Methods*, 2002.

2   P. Vogel and K. N. Houk, *Organic Chemistry: Theory, Reactivity and Mechanisms in Modern Synthesis*, Wiley, 2019.

3   S. Sankararaman, *Pericyclic Reactions – A Textbook: Reactions, Applications and Theory*, Wiley, Weinheim, 2005.

4   J. Sauer, *Angew. Chemie Int. Ed. English*, 1967, **6**, 16–33.

5   I. Fleming, *Molecular Orbitals and Organic Chemical Reactions*, Wiley, Chichester, 2009.

6   K. N. Houk, *J. Am. Chem. Soc.*, 1973, **95**, 4092–4094.

7   K. N. Houk, *Acc. Chem. Res.*, 1975, **8**, 361–369.

8   L. R. Domingo, M. J. Aurell, P. Pérez and R. Contreras, *J. Phys. Chem. A*, 2002, **106**, 6871–6875.

9   B. J. Levandowski, T. A. Hamlin, F. M. Bickelhaupt and K. N. Houk, *J. Org. Chem.*, 2017, **82**, 8668–8675.

10   F. M. Bickelhaupt and K. N. Houk, *Angew. Chem., Int. Ed.*, 2017, **56**, 10070.

11   L. P. Wolters and F. M. Bickelhaupt, *Wiley Interdisc. Rev. Comput. Mol. Sci.*, 2015, **5**, 324–343.

12   I. Fernández, *European J. Org. Chem.*, 2018, **2018**, 1394–1402.

13   Y. García-Rodeja, M. Solà, F. M. Bickelhaupt and I. Fernández, *Chem. - A Eur. J.*, 2017, **23**, 11030–11036.

14   E. Picazo, K. N. Houk and N. K. Garg, *Tetrahedron Lett.*, 2015, **56**, 3511–3514.

15   D. H. Ess and K. N. Houk, *J. Am. Chem. Soc.*, 2007, **129**, 10646–10647.

16   G. Frenking and F. Matthias Bickelhaupt, in *The Chemical Bond*, Wiley-VCH Verlag GmbH & Co. KGaA, Weinheim, Germany, 2014, pp. 121–157.

17   B. Wu, Z. Yu, X. Gao, Y. Lan and Y. G. Zhou, *Angew. Chemie - Int. Ed.*, 2017, **56**, 4006–4010.

18   M. Yamanaka, K. Sakata, K. Yoshioka, D. Uraguchi and T. Ooi, *J. Org. Chem.*, 2017, **82**, 541–548.

19   H. Ni, Z. Yu, W. Yao, Y. Lan, N. Ullah and Y. Lu, *Chem. Sci.*, 2017, **8**, 5699–5704.

20   F. Schoenebeck and K. N. Houk, *J. Am. Chem. Soc.*, 2010, **132**, 2496–2497.

21   J. L. Yu, S. Q. Zhang and X. Hong, *J. Am. Chem. Soc.*, 2017, **139**, 7224–7243.

22   Y. Li, C. Shan, Y. F. Yang, F. Shi, X. Qi, K. N. Houk and Y. Lan, *J. Phys. Chem. A*, 2017, **121**, 4496–4504.

23   D. H. Ess and K. N. Houk, *J. Am. Chem. Soc.*, 2007, **129**, 10646–10647.

24   I. Fernández and G. Frenking, *European J. Org. Chem.*, 2019, **2019**, 478–485.

25   I. Fernández and F. M. Bickelhaupt, *Chem. - An Asian J.*, 2016, **11**, 3297–3304.

26   M. Chen, C. Q. He and K. N. Houk, *J. Org. Chem.*, 2019, **84**, 1959–1963.

27   C. E. A. Sousa, A. M. P. Ribeiro, A. Gil Fortes, N. M. F. S. A. Cerqueira and M. J. Alves, *J. Org. Chem.*, 2017, **82**, 982–991.

28   F. Schoenebeck, D. H. Ess, G. O. Jones and K. N. Houk, *J. Am. Chem. Soc.*, 2009, **131**, 8121–8133.

29   I. Fernández and F. M. Bickelhaupt, *J. Comput. Chem.*, 2014, **35**, 371–376.

30   A. M. Sarotti, *Org. Biomol. Chem.*, 2014, **12**, 187–199.

31   J. J. Cabrera-Trujillo and I. Fernández, *Org. Biomol. Chem.*, 2019, **17**, 2985–2991.

32   J. Andrés, P. W. Ayers, R. A. Boto, R. Carbó-Dorca, H.

Chermette, J. Cioslowski, J. Contreras-García, D. L. Cooper, G. Frenking, C. Gatti, F. Heidar-Zadeh, L. Joubert, Á. Martín Pendás, E. Matito, I. Mayer, A. J. Misquitta, Y. Mo, J. Pilmé, P. L. A. Popelier, M. Rahm, E. Ramos-Cordoba, P. Salvador, W. H. E. Schwarz, S. Shahbazian, B. Silvi, M. Solà, K. Szalewicz, V. Tognetti, F. Weinhold and É. Zins, *J. Comput. Chem.*, 2019, **40**, 2248–2283.

33   B. J. Levandowski, T. A. Hamlin, R. C. Helgeson, F. M. Bickelhaupt and K. N. Houk, *J. Org. Chem.*, 2018, **83**, 3164–3170.

34   W. J. Van Zeist and F. M. Bickelhaupt, *Org. Biomol. Chem.*, 2010, **8**, 3118–3127.

35   F. Liu, Y. Liang and K. N. Houk, *Acc. Chem. Res.*, 2017, **50**, 2297–2308.

36   I. Fernández and F. M. Bickelhaupt, *Chem. Soc. Rev.*, 2014, **43**, 4953.

37   A. Artigas, I. Fernández and M. Solà, *J. Org. Chem.*, 2019, **84**, 9017–9024.

38   Y. García-Rodeja, M. Solà and I. Fernández, *J. Org. Chem.*, 2018, **83**, 3285–3292.

39   D. H. Ess, G. O. Jones and K. N. Houk, *Adv. Synth. Catal.*, 2006, **348**, 2337–2361.

40   J. M. Medina, J. L. MacKey, N. K. Garg and K. N. Houk, *J. Am. Chem. Soc.*, 2014, **136**, 15798–15805.

41   D. H. Ess, G. O. Jones and K. N. Houk, *Org. Lett.*, 2008, **10**, 1633–1636.

42   D. H. Ess and K. N. Houk, *J. Am. Chem. Soc.*, 2008, **130**, 10187–10198.

43   Y. Zhao and D. G. Truhlar, *Theor. Chem. Acc.*, 2008, **120**, 215–241.

44   F. Weigend and R. Ahlrichs, *Phys. Chem. Chem. Phys.*, 2005, **7**, 3297.

45   M. J. Frisch, G.W.Trucks, H. B. Schlegel, G. E.Scuseria, M. A. Robb, J. R. Cheeseman, G. Scalmani, V. Barone, B. Mennucci, G. A. Petersson, H. Nakatsuji, M. Caricato, X. Li, H. P. Hratchian, A. F. Izmaylov, J. Bloino, G. Zheng, J. L. Sonnenberg, M. Hada, M. Ehara, K. Toyota, R. Fukuda, J. Hasegawa, M. Ishida, T. Nakajima, Y. Honda, O. Kitao, H. Nakai, T. Vreven, J.A.Montgomery, J.E.Peralta, F.Ogliaro, M. Bearpark, J. J. Heyd, E. Brothers, K.N. Kudin, V. N. Staroverov, R. Kobayashi, J. Normand, K. Raghavachari, A. Rendell, J. C. Burant, S. S. Iyengar, J. Tomasi, M. Cossi, N. Rega, J. M.Millam, M. Klene, J. E. Knox, J.B.Cross, V. Bakken, C.Adamo, J.Jaramillo, R. Gomperts, R. E. Stratmann, O. Yazyev, A.J.Austin, R. Cammi, C. Pomelli, J. W. Ochterski, R. L. Martin, K.Morokuma, V.G.Zakrzewski, G. A. Voth, P.Salvador, J. J. Dannenberg, S.Dapprich, A. D. Daniels, Ö. Farkas, J. B. Foresman, J. V. Ortiz, J. Cioslowski and D. J. Fox, *Gaussian 09, Revision C.01*, Gaussian, Inc., Wallingford CT, 2009.

46   E. J. Baerends, J. Autschbach, A. Berces, J. A. Berger, F. M. Bickelhaupt, C. Bo, P. L. de Boeij, P. M. Boerrigter, L. Cavallo, D. P. Chong, L. Deng, R. M. Dickson, D. E. Ellis, M. van Faassen, L. Fan, T. H. Fischer, C. Fonseca Guerra, S. J. A. van Gisbergen, J. A. Groeneveld, O. V. Gritsenko, M. Grüning, F. E. Harris, P. van den Hoek, C. R. Jacob, H. Jacobsen, L. Jensen, E. S. Kadantsev, G. van Kessel, R.

Klooster, F. Kootstra, E. van Lenthe, D. A. McCormack, A. Michalak, J. Neugebauer, V. P. Nicu, V. P. Osinga, S. Patchkovskii, P. H. T. Philipsen, D. Post, C. C. Pye, W. Ravenek, P. Romaniello, P. Ros, P. R. T. Schipper, G. Schreckenbach, J. Snijders, M. Solà, M. Swart, D. Swerhone, G. te Velde, P. Vernooijs, L. Versluis, L. Visscher, O. Visser, F. Wang, T. A. Wesolowski, E. M. van Wezenbeek, G. Wiesenekker, S. K. Wolff, T. K. Woo, A. L. Yakovlev, T. Ziegler, Computer Code ADF 2016.01; Scientific Computing and Modeling NV: Amsterdam, The Netherlands http://www.scm.com.

47   CYLview, 1.0b; Legault, C. Y., Université de Sherbrooke, 2009 (http://www.cylview.org)

48   G. Schill, C. U. Priester, U. F. Windhövel and H. Fritz, *Tetrahedron*, 1987, **43**, 3765–3786.

49   R. Sustmann, S. Tappanchai and H. Bandmann, *J. Am. Chem. Soc.*, 1996, **118**, 12555–12561.

50   T. A. Hamlin, D. Svatunek, S. Yu, L. Ridder, I. Infante, L. Visscher and F. M. Bickelhaupt, *European J. Org. Chem.*, 2019, **2019**, 378–386.

51   S. Danishefsky, T. Kitahara, C. F. Yan and J. Morris, *J. Am. Chem. Soc.*, 1979, **101**, 6996–7000.

52   K. et al., *Izv. Akad. Nauk SSSR. Seriya khimicheskaya.*, 1959, 682.

ARTICLE

72x15mm (600 x 600 DPI)